



Single Crystal X-ray Structure Analyses of Thallides: Halide Incorporation and Mixed Alkali Sites in $A_8Tl_{11}X$ ($A = K, Rb, Cs$; $X = Cl, Br$)[†]

Stefanie Gärtner^{1,2,*} and Susanne Tiefenthaler¹

¹ Institute of Inorganic Chemistry, University of Regensburg, 93040 Regensburg, Germany; susanne.tiefenthaler@ur.de

² Central Analytics (X-Ray Dept.), University of Regensburg, 93040 Regensburg, Germany

* Correspondence: stefanie.gaertner@ur.de; Tel.: +49-941-943-4446

† Presented at the 1st International Electronic Conference on Crystals, 21–31 May 2018. Available online: https://sciforum.net/conference/IECC_2018.

Published: 21 May 2018

Abstract: A_8Tl_{11} (A = alkali metal) compounds have been known since the investigations of Corbett et al. in 1995 and still are matter of current discussions as the compound includes one extra electron referred to the charge of the Tl_{11}^{7-} cluster. Attempts to substitute the charge by incorporation of a halide atom succeeded for the lightest homologue of the group, $Cs_8Ga_{11}Cl$, and powder diffraction experiments for the heavier homologues also suggested the formation of analogous compounds. However, X-ray single crystal studies on $A_8Tl_{11}X$ to prove this substitution and to provide a deeper insight into the influence on the thallide substructure have not yet been performed, probably due to severe absorption combined with air and moisture sensitivity for this class of compounds. In our contribution we present single crystal X-ray analyses of the new compounds $Cs_8Tl_{11}Cl_{0.8}$, $Cs_8Tl_{11}Br_{0.9}$ and $Cs_5Rb_3Tl_{11}Cl_{0.5}$. It is shown that a (partial) incorporation of halide can also be indirectly determined by examination of the Tl–Tl distances for low resolved data sets, e.g., for $Cs_{5.7}K_{2.3}Tl_{11}Cl_7$. Mixed occupied sites by two different alkali metals indicate a dependence on the cesium content, the systems K/Rb–Tl–Br and K/Rb–Tl–Cl only gave rise to the formation of the higher reduced $(K/Rb)_8Tl_{11}$ and the less reduced by-product $(K/Rb)_{15}Tl_{27}$. We have not been able to prove the formation of halide including thallides in the absence of cesium.

Keywords: thallides; X-ray structure analysis; intermetallics

1. Introduction

The largest (empty) thallide cluster is represented by the Tl_{11}^{7-} cluster which is present in binary materials A_8Tl_{11} [1,2] and $A_{15}Tl_{27}$ [3] ($A = K, Rb, Cs$). The A_8Tr_{11} structure type was first described in 1991 for the lighter homologue indium in K_8In_{11} , [1,4] of which the crystal structure proved the presence of a naked, pentacapped trigonal prismatic shaped In_{11} cluster, which was assigned a charge of -7 . Additionally, one extra-electron per formula unit is present, which is responsible for the metallic character. The additional electron, referred to the charge of -7 of the cluster anion, is not necessary for the stability of the clusters [5] and can be replaced by halide atoms, which are located on a $\bar{3}$ void (Wyckoff position $6b$) at the origin of the unit cell resulting in a diamagnetic character of the compounds. Halide incorporation was proven for the lighter homologue of the group, $Cs_8Ga_{11}Cl$ by X-ray single crystal structure analysis. [6] Powder diffraction experiments suggested the formation of the heavier homologues $Rb_8Ga_{11}Cl$, $Cs_8Ga_{11}X$ ($X = Br, I$), $Rb_8In_{11}Cl$, $Cs_8In_{11}Cl$, $Cs_8Tl_{11}X$ ($X = Cl, Br, I$). The formation of $Rb_8Tl_{11}Cl$ was termed as doubtful due to the lack of a significant change in the lattice constants compared to Rb_8Tl_{11} .

The questions we wanted to answer were: (1) How does the geometry of the thallide cluster change on halide incorporation; (2) Is there a $\text{Rb}_3\text{Tl}_{11}\text{Cl}$?; (3) How do mixed cation sites affect the amount of halide incorporation?

In Section 2 (Results) we report on the first single crystal X-ray structure determination of halide including thallides, $\text{Cs}_8\text{Tl}_{11}\text{Cl}_{0.8}$, $\text{Cs}_8\text{Tl}_{11}\text{Br}_{0.9}$, $\text{Cs}_5\text{Rb}_3\text{Tl}_{11}\text{Cl}_{0.5}$ and $\text{Cs}_{5.7}\text{K}_{2.3}\text{Tl}_{11}\text{Cl}_{0.6}$. Subsequently, (Section 3, Discussions) the crystal structures are investigated according to the questions listed above.

2. Results

All compounds crystallize in a variant of the K_3In_{11} structure type (rhombohedral, spacegroup $R\bar{3}c$) and especially for the mixed alkali metal compounds, many of the crystals happened to form typical “multicrystals”. Due to the presence of reverse/obverse twinning a $R(\text{obv})$ filter was applied during data reduction. The materials naturally possess very high absorption coefficients ($\mu > 60 \text{ mm}^{-1}$), therefore small single crystals have been chosen for the X-ray analyses. However, the data sets still suffer from severe absorption effects which could be reduced by carefully applying numerical absorption correction (including refinement of A and B factors). Thereby, the adjustment of the correct shape played a dominant role. Table 1 lists selected data for the structure determination. For the chloride including compounds two additional, unresolved but several times reproduced residual electron density peaks ($\approx 1.5 \text{ \AA}$ beside the chlorine atom, $\approx 2.2 \text{ \AA}$ beside cesium; along the c -axis) are present, which we attribute to unresolved absorption effects as this direction is along the thinnest direction of the plate like crystals. For the bromine including compound this effect is not as dominant as for the chlorine including ones but still is observed.

Table 1. Selected data reduction and refinement details.

Chemical Formula	$\text{Cs}_8\text{Tl}_{11}\text{Cl}_{0.8}$	$\text{Cs}_8\text{Tl}_{11}\text{Br}_{0.9}$	$\text{Cs}_5\text{Rb}_3\text{Tl}_{11}\text{Cl}_{0.5}$	$\text{Cs}_{5.7}\text{K}_{2.3}\text{Tl}_{11}\text{Cl}_{0.6}$
Space group	$R\bar{3}c$	$R\bar{3}c$	$R\bar{3}c$	$R\bar{3}c$
a [Å]	10.4697(4)	10.5608(3)	10.3791(5)	10.3291(9)
b [Å]	10.4691(4)	10.5608(3)	10.3791(5)	10.3291(9)
c [Å]	53.297(3)	53.401(2)	52.437(3)	51.909(5)
α [°]	90	90	90	90
β [°]	90	90	90	90
γ [°]	120	120	120	120
V [Å ³]	5058.8(5)	5157.9(4)	4892.0(5)	4796.3(9)
μ [mm ^{−1}]	60.902	60.745	64.052	61.908
R indices (all data)	$R1 = 0.0309$, $wR2 = 0.0629$	$R1 = 0.0280$, $wR2 = 0.0541$	$R1 = 0.0466$, $wR2 = 0.0970$	$R1 = 0.0566$, $wR2 = 0.1034$
R_{int}	0.0497	0.0385	0.0446	0.0449

With only one cation being present in the $\text{Cs}_8\text{Tl}_{11}\text{Cl}_{0.8}$ and $\text{Cs}_8\text{Tl}_{11}\text{Br}_{0.9}$, phase pure materials could be obtained according to the powder diffraction pattern of the bulk material (refined cell constants at room temperature for $\text{Cs}_8\text{Tl}_{11}\text{Cl}_{0.8}$: $a = 10.566(5)$, $c = 53.67(3)$, $R\bar{3}c$, 17 single indexed lines, Figure 1). Additionally the unit cells were checked for several single crystals which confirmed phase pureness.

The quality of the crystals is significantly improved for $\text{Cs}_8\text{Tl}_{11}\text{X}$ compared to the mixed alkali metal compounds, and in these cases we were able to obtain better resolved data which allowed for the determination of split positions of one alkali metal according to the site occupancy factor (s.o.f.) of the halide atom. For the reported single crystals with mixed alkali metal positions the data quality is worse compared to $\text{Cs}_8\text{Tl}_{11}\text{X}$ phases, therefore the splitting of the alkali metal position could not be observed due to the lower resolution of the data sets. In this case, we refined the s.o.f. of the halide and for $\text{Cs}_5\text{Rb}_3\text{Tl}_{11}\text{Cl}_{0.5}$ this resulted in an improvement of the F_o/F_{calc} ratio and the residual electron density, therefore we consider the value of 0.50(4) to be true. In contrast, the same treatment of the halide in the data set of $\text{Cs}_{5.7}\text{K}_{2.3}\text{Tl}_{11}\text{Cl}_{0.6}$ (refined s.o.f.: 0.60(4)) did not allow for a significant

improvement of the model, therefore the amount of halide incorporation cannot be determined reliably in this case, but the s.o.f. value of the halogen atom fits the s.o.f. for Cs amount of the split position.

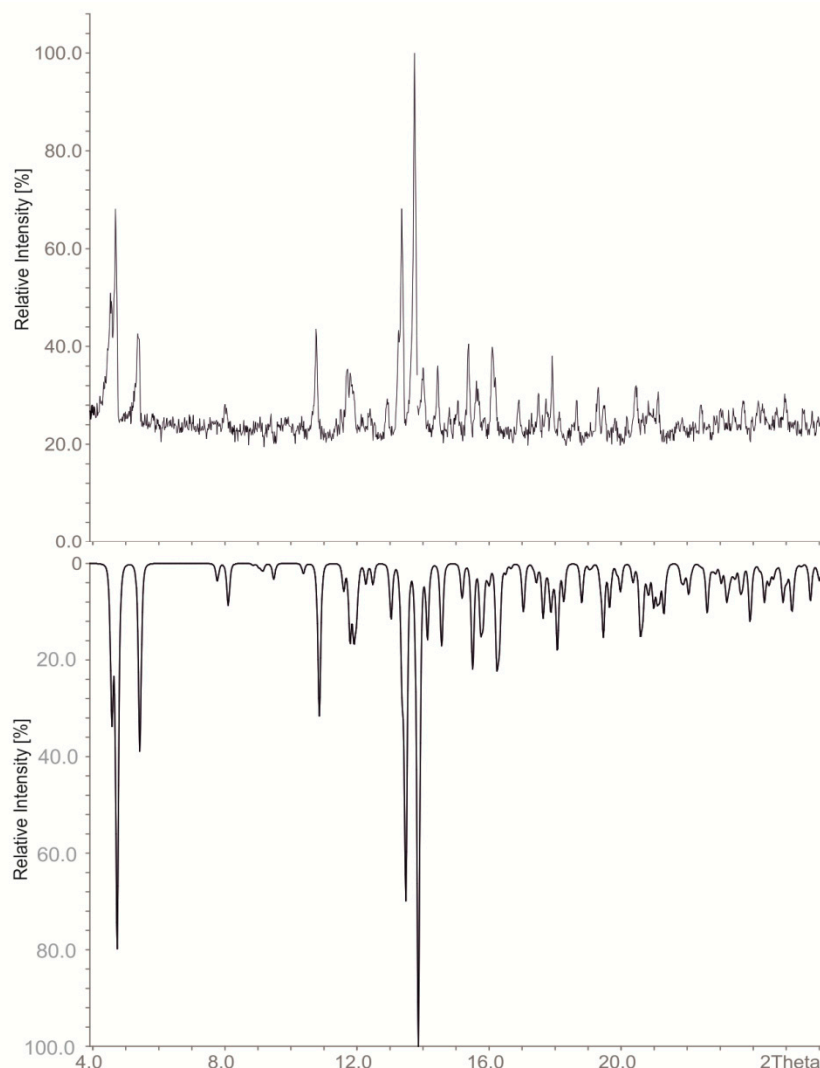


Figure 1. Powder diffraction patterns of $\text{Cs}_8\text{Tl}_{11}\text{Cl}_{0.8}$: Measured (**top**) and calculated (**bottom**; calculated from single crystal data of $\text{Cs}_8\text{Tl}_{11}\text{Cl}_{0.8}$).

3. Discussion

3.1. How Does the Geometry of the Thallide Cluster Change on Halide Incorporation?

All A_8Tl_{11} and $\text{A}_8\text{Tl}_{11}\text{X}_x$ compounds include Tl_{11}^{7-} clusters, which are best described as a very compressed, pentacapped trigonal prism [2]. Three symmetry independent thallium atoms are located on three different Wyckoff positions of space group $R\bar{3}c$: Tl1(12c; 3-fold rotational axis), Tl2 (36f; general position) and Tl3 (18e; 2-fold rotational axis) and build up a cluster consisting of 11 Tl atoms in point group D_{3h} . The deviations from point group D_{3h} are very small (Figure 2) and are represented by a distortion of the height of the trigonal prism built by Tl3-atoms. This distortion is also reflected in the distances of Tl2-Tl3 ($d(\text{Tl2-Tl3}) = cd$) as there are two crystallographically independent distances present. The degree of distortion decreases with increasing similarity of the capping distances (cd). In Tables 2 and 3 the distances as well as the distortion angles are listed and the dependence on the amount of halide incorporation is clearly evident. In contrast, the height of the trigonal prism (Tl3-Tl3) as well as the distance of the capping atom Tl2 to the mean plane built by Tl3 atoms [$d(\text{Tl2-plane}) = 0.56 \text{ \AA}$] and also the Tl1-Tl3 distances do not significantly change. Based on

these observations we introduce a cdd/cd_{av} ratio (cdd : capping distance difference; cd_{av} : average capping distance; (1)) which allows for a quick estimation of the degree of distortion.

Table 2. Selected distances (numbering scheme according to Figure 2, values taken from [1,2]), tilt angle and cdd/cd_{av} value for K_8Tl_{11} and Rb_8Tl_{11} .

		K_8Tl_{11}	Rb_8Tl_{11}
Tl2	Tl3	3.0476(4)	3.060
Tl2	Tl3 ³	3.1396(4)	3.157
Tl1	Tl3 ¹	3.1304(4)	3.147
Tl3	Tl3 ³	3.2054(7)	3.219
Tilt		4.69(2)°	4.90°
cdd/cd_{av} [%]		3.0	3.1

^{1,3} symmetry operations according to Figure 2

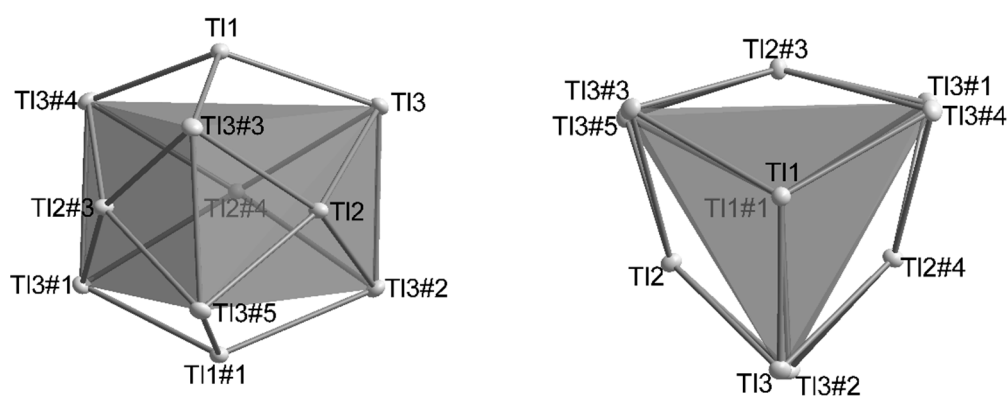


Figure 2. The distortion of the trigonal prism in the Tl_{11}^{7-} results in the point group D_3 for the cluster. Symmetry operations for the generation of equivalent atoms: #1: $1/3 + x - y, 2/3 - y, 7/6 - z$; #2: $1/3 + y, -1/3 + x, 7/6 - z$; #3: $1 - y, x - y, z$; #4: $1 - x + y, 1 - x, z$; #5: $4/3 - x, 2/3 - x + y, 7/6 - z$.

Table 3. Selected distances (numbering scheme according to Figure 2), tilt angle and cdd/cd_{av} value for $Cs_8Tl_{11}Cl_{0.8}$, $Cs_8Tl_{11}Br_{0.9}$, $Cs_5Rb_3Tl_{11}Cl_{0.5}$ and $Cs_{5.7}K_{2.3}Tl_{11}Cl_7$.

		$Cs_8Tl_{11}Cl_{0.8}$	$Cs_8Tl_{11}Br_{0.9}$	$Cs_5Rb_3Tl_{11}Cl_{0.5}$	$Cs_{5.7}K_{2.3}Tl_{11}Cl_{0.6}$
Tl2	Tl3	3.0656(4)	3.0743(2)	3.0605(6)	3.0554(7)
Tl2	Tl3 ³	3.0632(4)	3.0766(2)	3.0896(6)	3.0656(4)
Tl1	Tl3 ¹	3.0894(4)	3.1006(2)	3.1049(7)	3.0884(8)
Tl3	Tl3 ³	3.2019(11)	3.2102(4)	3.2025(11)	3.1873(11)
Tilt [°]		0.12(2)	0.069(7)	0.94(2)	0.34(5)
cdd/cd_{av} [%]		0.1	0.1	0.9	0.4

3.2. Is There a $Rb_8Tl_{11}Cl$?

Despite numerous efforts we did not succeed in synthesizing $Rb_8Tl_{11}Cl$ and the analogous reaction approaches only yielded crystals of Rb_8Tl_{11} of bad quality. The incorporation of halide cannot be completely ruled out as there is some residual electron density at Wyckoff position 6b according to the position of the halide atom in the previously discussed compounds. However, the cdd/cd_{av} ratio of 2.4% compared to 3.0 % (K_8Tl_{11}) and 3.1% (Rb_8Tl_{11}) and a tilt angle of 2.4° (K_8Tl_{11} : 4.7°, Rb_8Tl_{11} : 4.9°) suggest a minimal involvement of chloride; the s.o.f. for chlorine at this position refined to a value of 10%, but the resolution of the data set does not allow for a distinct statement.

3.3. How Do Mixed Cation Sites Affect the Amount of Halide Incorporation?

It needs to be emphasized that for the preparation of all compounds the same stoichiometric approach was employed and the dependence of the amount of halide incorporation on the cesium content is conspicuous. Therefore, the cation positions need to be examined more in detail. There are two different cation positions in the asymmetric unit corresponding to Wyckoff position $36f$ for A1 and Wyckoff position $12c$ for A2. For $\text{Cs}_5\text{Rb}_3\text{Tl}_{11}\text{Cl}_{0.5}$ and $\text{Cs}_{5.7}\text{K}_{2.3}\text{Tl}_{11}\text{Cl}_7$ the position of A1 is mixed occupied by both alkali metals and the s.o.f. values for cesium on the mixed position are very similar to the s.o.f. for the halide, although the value of 0.60(4) for $\text{Cs}_{5.7}\text{K}_{2.3}\text{Tl}_{11}\text{Cl}_7$ cannot be affirmed definitely. The position of A2 is only occupied by the heavier alkali metal cesium, which is in accordance with the observations of Corbett et al. for the A_8Tl_{11} phases. [2] This cation position shows the previously mentioned splitting dependent on the s.o.f. of the halogen atom. The resulting coordination sphere of the halide is best described as distorted cubic, where the longer distances are along the room diagonal of the cubic arrangement from the halide to the position of A2. This distance shortens significantly for X-A2 by the introduction of the split positions (same s.o.f. as halide), resulting in a less distorted cubic arrangement (Figure 3). This might explain the observation, that halides are only incorporated when cesium occupies A2 and is also involved in A1 mixed occupied sites, as the (distorted) cubic arrangement resembles very much the coordination of the halide in the CsCl structure type ($d(\text{Cs}-\text{Cl}) = 3.573 \text{ \AA}$; $d(\text{Cs}-\text{Br}) = 3.718 \text{ \AA}$).

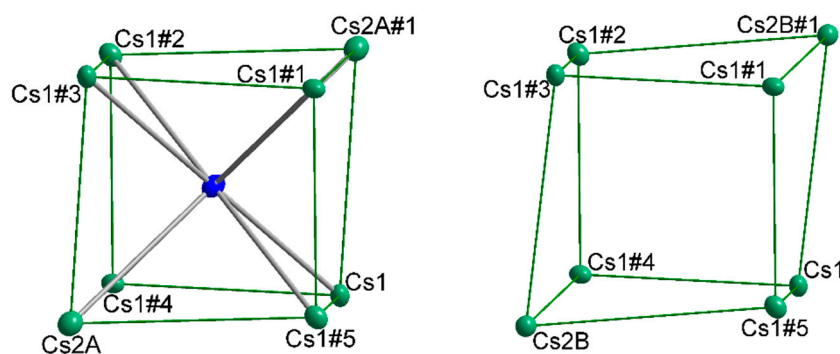


Figure 3. Distorted cubic arrangement around the halide, respectively void. Cs1: x, y, z ; Cs1#1: $1 - y, x - y, z$; Cs1#2: $1 - x + y, 1 - x, z$; Cs1#3: $4/3 - x, 2/3 - y, 2/3 - z$; Cs1#4: $1/3 + y, 2/3 - x + y, 2/3 - z$; Cs1#5: $1/3 + x - y, -1/3 + x, 2/3 - z$; Cs2A/B: x, y, z ; Cs2A/B#1: $4/3 - x, 2/3 - y, 2/3 - z$.

The previously stated stability of the halide including $\text{A}_8\text{Tl}_{11}\text{X}$ phases might not be exclusively caused by the effect of charge balance due to halide incorporation but additionally by the stabilization of halide in a distorted cubic arrangement (Figure 4). This might also explain that less (or even no) halide is incorporated when less (or no) cesium is involved. In return, the Tl_{11} clusters themselves seem to tolerate any charge between 7^- and 8^- .

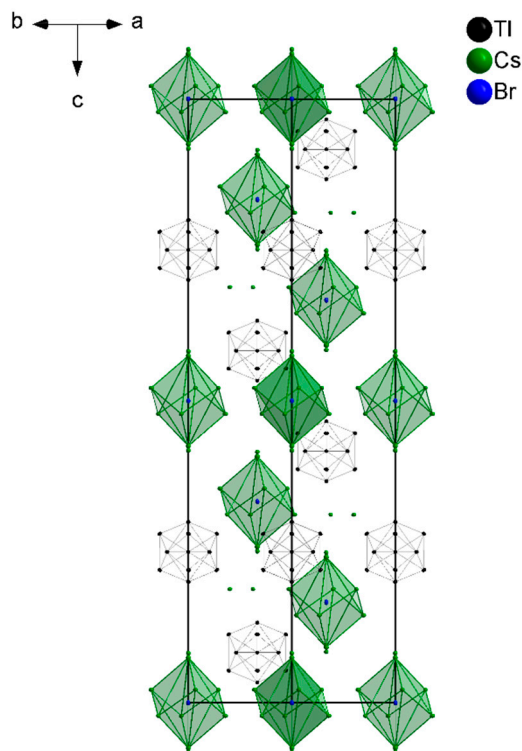


Figure 4. The unit cell of $\text{Cs}_8\text{Tl}_{11}\text{Br}_{0.9}$ shows the two characteristic components: Tl_{11} clusters and the distorted cubic arrangement around the halide atom.

4. Materials and Methods

All compounds have been synthesized via a stoichiometric approaches using high temperature solid state techniques. Cesium and Rubidium were produced by the reduction of the corresponding alkali metal halide with elemental Calcium [7] and distilled twice, potassium was segregated for purification. Thallium lumps have been stored under inert atmosphere and were used without further purification. The starting materials were enclosed in tantalum crucibles which were subsequently placed in quartz glass ampoules and sealed under argon atmosphere. The same temperature program was used for all compounds: Heating to 700 °C with a heating rate of 50 °C/h, holding for 24 h, cooling to room temperature with a cooling rate of 3 °C/h to allow for crystallization. All compounds are very sensitive towards moisture and oxygen and degeneration of the crystals was observed (gassing) in dried mineral oil within a few hours. Suitable single crystals for X-ray structure analysis were isolated in dried mineral oil and mounted on an Agilent SuperNova (Mo-source, Eos detector) using MiTeGen loops. Thereby, the transfer needed to be very quick as the crystals started to decompose as soon as the mineral oil film became too thin. Once placed on the diffractometer in the nitrogen stream at 123 K the crystals remained stable and data collection was possible.

Author Contributions: S.G. conceived and designed the experiments; S.G. and S.T. performed the experiments; S.G. and S.T. wrote the paper.

Acknowledgments: The authors thank N. Korber for supplying materials and helpful discussions and M. Schlosser for executing powder diffraction experiments.

Conflicts of Interest: The authors declare no conflict of interest.

References

1. Blase, W.; Cordier, G.; Muller, V.; Haussermann, U.; Nesper, R.; Somer, M. Präparation und Kristallstrukturen von $\text{Rb}_8\text{In}_{11}$, K_8Tl_{11} und $\text{Rb}_8\text{Tl}_{11}$ sowie Bandstrukturechnungen zu K_8In_{11} . *Z. Naturforsch. Sect. B* **1993**, *48*, 754–760.
2. Dong, Z.-C.; Corbett, J.D. A_8Tl_{11} ($\text{A} = \text{K}, \text{Rb}$ or Cs) Phases with Hypoelectronic Tl_{11}^{7-} Cluster Anions: Syntheses, Structure, Bonding and Properties. *J. Clust. Sci.* **1995**, *6*, 187–201.
3. Dong, Z.C.; Corbett, J.D. $\text{A}_{15}\text{Tl}_{27}$ ($\text{A} = \text{Rb}, \text{Cs}$): A Structural Type Containing Both Isolated Clusters and Condensed Layers Based on the Tl_{11} Fragment. Syntheses, Structure, Properties, and Band Structure. *Inorg. Chem.* **1996**, *35*, 1444–1450.
4. Sevov, S.C.; Corbett, J.D. A Remarkable Hypoelectronic Indium Cluster in K_8In_{11} . *Inorg. Chem.* **1991**, *30*, 4875–4877.
5. Wang, F.; Wedig, U.; Prasad, D.; Jansen, M. Deciphering the Chemical Bond in Anionic Thallium Clusters. *J. Am. Chem. Soc.* **2012**, *134*, 19884–19894.
6. Henning, R.W.; Corbett, J.D. $\text{Cs}_8\text{Ga}_{11}$, a New Isolated Cluster in a Binary Gallium Compound. A Family of Valence Analogues $\text{A}_8\text{Tr}_{11}\text{X}$: $\text{A} = \text{Cs}, \text{Rb}$; $\text{Tr} = \text{Ga}, \text{In}, \text{Tl}$; $\text{X} = \text{Cl}, \text{Br}, \text{I}$. *Inorg. Chem.* **1997**, *36*, 6045–6049.
7. Hackspill, L. Sur quelques propriétés des métaux alcalins. *Helv. Chim. Acta* **1928**, *11*, 1003–1026.



© 2018 by the authors. Licensee MDPI, Basel, Switzerland. This article is an open access article distributed under the terms and conditions of the Creative Commons Attribution (CC BY) license (<http://creativecommons.org/licenses/by/4.0/>).